ATMOSPHERIC ENVIRONMENT: X 14 (2022) 100173

Contents lists available at ScienceDirect

Atmospheric Environment: X

journal homepage: www.journals.elsevier.com/atmospheric-environment-x

Evaluation of modelled LOTOS-EUROS with observational based PM10 source attribution

R. Timmermans [a,*], D. van Pinxteren [b], R. Kranenburg [a], C. Hendriks [a,1], K.W. Fomba [b], H. Herrmann [b], M. Schaap [a,c]

[a] The Netherlands Organisation for Applied Scientific Research (TNO), Climate, Air and Sustainability Department, Princetonlaan 6, 3584 CB, Utrecht, the Netherlands
[b] Leibniz Institute for Tropospheric Research (TROPOS), Atmospheric Chemistry Department (ACD), Permoserstr. 15, 04318, Leipzig, Germany
[c] Freie Universität Berlin (FUB), Institute of Meteorology, Berlin Carl-Heinrich-Becker-Weg 6–10, 12165, Berlin, Germany

ARTICLE INFO

Keywords:
Source attribution
Air pollution
Chemistry transport model
Germany
Particulate matter
PMF

ABSTRACT

Due to its serious health impact particulate matter is one of the air pollutants subject to abatement policies. Information on the main sources responsible for high concentrations of pollutants is therefore crucial to enable effective policy measures. In this study we compared two different methods for attribution of particulate matter concentrations to different sources: A tagging approach within the regional chemistry transport model LOTOS-EUROS and an observational method using speciated particulate matter observations and Positive Matrix Factorisation (PMF). The methods have been applied for winter 2016/2017 over Eastern Germany where in wintertime high woodburning emissions, cold temperatures and regular easterly winds can lead to a build-up of pollutant concentrations. The comparison allows the validation of the modelled source attribution for a selection of source categories. The contributions for biomass and total combustion compare well between both methods providing trust in the determined contributions, applied emissions including their timing. The total contribution from combustion is estimated between 3.3-7.7 μg/m^3 (PMF) and 3.3-7.2 μg/m^3 (LOTOS-EUROS) for the 9 stations incorporated in the study. The temporal Pearson correlation coefficient ranges between 0.3-0.64 for total combustion and 0.34 and 0.7 for biomass combustion. The mean absolute contributions for traffic at background stations also compare well with most values between 1.5-2.0 μg/m^3 for PMF and 1–1.6 μg/m^3 for LOTOS-EUROS. A lack of correlation for this contribution however suggests that the model has difficulty in representing the source category traffic in a time consistent manner and developments are needed to improve the temporal distribution of the traffic emissions within the model. The modelled particulate matter concentrations displayed a 20–40% underestimation of the observed concentrations with an increasing bias during high pollution events. The underestimation showed a high correlation with the observed contribution from combustion and secondary particulate matter including ammonium sulfate and organic carbon suggesting that at least a part of the missing mass in LOTOS-EUROS is related to transformation of volatile combustion emissions, likely from solid fuels, to secondary particle mass and missing enhanced formation of sulfate. Implementation of these missing processes would help to improve the source attribution of particulate matter with the LOTOS-EUROS model.

1. Introduction

Air pollution is the number fourth leading cause of deaths worldwide, with an estimated amount of 6.67 million deaths in 2019, from which 4.7 are attributed to outdoor air pollution (HEI, 2020).

Particulate matter (PM) is believed to be the main air pollutant responsible for the negative health effects associated to air pollution. To protect human health the EU air quality directive has set limit values for particulate matter concentrations (https://ec.europa.eu/environment/air/quality/standards.htm). Based on health risk assessments the World Health Organisation (WHO) has further recommended stricter limit values of 15 and 5 μm/m^3 for the yearly averaged PM10 and PM2.5 respectively (WHO, 2021). Around 91% of the world's population in 2019 lived in places where the air quality levels exceeded the previous

* Corresponding author. Princetonplein 6, Utrecht, the Netherlands.
E-mail address: renske.timmermans@tno.nl (R. Timmermans).
[1] Now at Radboud Centre for Sustainability Challenges, Nijmegen, the Netherlands.

https://doi.org/10.1016/j.aeaoa.2022.100173
Received 13 January 2022; Received in revised form 11 April 2022; Accepted 13 April 2022
Available online 18 April 2022

recommended WHO limit of 10 μm/m^3 PM2.5. With the newest reduced air quality guideline level of 5 μm/m^3, this will be even higher.

To be able to design effective policy measures with the aim to meet the limit values, it is crucial to know which source sectors and regions are responsible for high concentrations of particulate matter. To identify the spatial origin of air pollution, different types of models, such as chemistry transport models or back trajectory models, can be used. Also, for the identification of the responsible source sectors (e.g. traffic, industry, residential combustion) there are different approaches available. There is the application of receptor modelling (RM) (see e.g. Belis et al., 2019, 2013; Hopke and Cohen, 2011; Viana et al., 2008) (such as Positive Matrix Factorisation (PMF)), which is observation-based. This type of models looks for internal correlation in the observation data, usually on a PM-component level. This analysis yields several factors that in some cases can be attributed to source categories. A different approach to determining the origin of the PM concentration in a certain location is to use chemistry transport modelling and gridded emission data (source-oriented models, SM). This is often done in scenario studies, in which the emissions from a sector or region are reduced one by one (Emission Reduction Impact (ERI) method or also called brute-force) to determine the source contribution to the total concentration for each source category (e.g. Amann et al., 2011; Huang et al., 2018; Thunis et al., 2018). Other models, such as LOTOS-EUROS, have installed a labelling (also called tagging) approach (Kranenburg et al., 2013; Wagstrom et al., 2008; Wang et al., 2009) to enable the quantification of source contributions for a number of source sectors/regions in one model run (Hendriks et al., 2013). The quality of the source apportionment information provided by chemistry transport models depend on the degree in which they reproduce the observed PM concentrations. Therefore, including a comparison with detailed PM composition observations is important to identify possible error sources in the model and assess the robustness of the source apportionment results.

Another way to assess the robustness of source apportionment results is to compare different methods. For the comparison with receptor models (based on observations) the labelling method is considered to be more suitable and comparable than the ERI/brute force methods (Mircea et al., 2020). Still this comparison is not straightforward and often hampered by differences in the source categories that are distinguished. It requires careful linking between the source factors in the RM and the source categories in the labelling approach. Especially the fact that secondary PM in RM is usually considered as separate factors and not attributed to specific source sectors hinders a direct comparison. This might also be the reason that only a few examples of comparisons or combined use of labelling/tagging versus receptor models can be found. Bove et al. (2014) compared results for 5 source categories from a tagging approach in the CAMx model to PMF source attribution in Genoa, Italy. They found that both methods agreed on the ranking of the main sources but that the required assumptions on the sources of secondary PM in the PMF led to larger uncertainties and discrepancies between both methods. Similarly Pirovano et al. (2015) also found an agreement on the ranking of the main sources when comparing results from the CAMx tagging method to another RM method: Chemical Mass Balance (CMB) in Lombardy, Italy. While a general agreement was found for the secondary inorganic aerosol contributions, large discrepancies were found for absolute contributions of the road traffic and residential heating sectors. For road traffic this was partly attributed to underestimated emissions at cold temperatures of organic carbon (OC) and precursors leading to secondary OC formation. Within the Forum for air quality MODEling (FAIRMODE) initiative a comparison was done for many different models (Belis et al., 2020), including also CTMs with labelling capacities and RM. The comparison between SM and RM focused on the area of Lens in France. They found that with RM the contribution from Industry was most difficult to determine as it showed largest variability. In most cases the contributions determined with SM [illegible] with RM. This is attributed to the un[illegible]ions by the models used for SM, mostly associated to problems with modelling the organic fraction. For the traffic-exhaust contribution and Industry the differences between the RM and SM results were smallest. Contrarily for soil and road dust the differences were largest, highlighting the need for improvement of these emissions in the models.

Within the present study, both a receptor modelling (PMF) and a chemistry transport modelling method are applied to quantify and compare the contributions of the main source sectors to the PM10 levels in eastern Germany. In this part of Germany exceedances of limit values often take place during cold and stable weather conditions with inflow of polluted air from other countries, such as Poland. This polluted air combined with the build-up of local air pollution in the shallow boundary layer can lead to high concentrations of PM10 and exceedances of limit values. The combined approach gives an opportunity to validate the modelled source attribution for a selection of source categories. While the LOTOS-EUROS source attribution system was part of the larger intercomparison by Belis et al. (2020) mentioned above for the city of Lens, France, it is important to evaluate the methodologies in different regions with varying pollution regimes and different source sector signatures. The availability of chemical speciation data and RM results for a network of 10 sites covering a large region enables to draw stronger conclusions and allows to distinguish between air pollution conditions and relative contributions representative for urban traffic, urban background and rural background locations.

The current study thus allows an evaluation of the current model version in combination with the anthropogenic emission data.

The applied PMF method requires an extensive set of observations of total PM as well as its components and several tracers (metals and organic compounds). This data set also gives the opportunity to zoom in to differences between modelled and observed concentrations, to identify which sources are not yet well represented in the emission data underlying the modelling calculations. Using this information, the emission data-base and chemistry transport model can be improved, leading to better source attribution.

2. Method & measurements

2.1. LOTOS-EUROS model

LOTOS-EUROS is an open-source 3D chemistry transport model. The model is developed at TNO in cooperation with partners from different institutes. The model is part of the Copernicus Atmospheric Monitoring (CAMS) regional ensemble providing operational forecasts and analyses over Europe. In this context the model is regularly updated and validated using observations from ground and satellite observations. In CAMS also policy products on source apportionment are provided using both the LOTOS-EUROS and EMEP models.

The LOTOS-EUROS model simulates air pollution concentrations in the lower troposphere on a regular Eulerian grid with variable resolution over Europe (Manders et al., 2017). The vertical grid can be adjusted according to the applied meteorological input data.

Gas-phase chemistry is simulated using the TNO CBM-IV scheme, which is a condensed version of the original scheme (Whitten et al., 1980). Hydrolysis of N_2O_5 is explicitly described (Schaap et al., 2004). LOTOS-EUROS explicitly accounts for cloud chemistry computing sulfate formation as a function of cloud liquid water content and cloud droplet pH (Banzhaf et al., 2012). For aerosol chemistry the thermodynamic equilibrium module ISORROPIA2 is used (Fountoukis and Nenes, 2007). Dry Deposition fluxes for gases are calculated using the resistance approach as implemented in the DEPAC (DEPosition of Acidifying Compounds) module (Van Zanten et al., 2010). Furthermore, a compensation point approach for ammonia is included in the dry deposition module (Wichink Kruit et al., 2012). For particles the scheme by Zhang (2001) is used. The wet deposition module accounts for droplet saturation (Banzhaf et al., 2012). The horizontal advection of pollutants is calculated applying a monotonic advection scheme

(Walcek, 2000). For a detailed description of the LOTOS-EUROS model we refer to (Manders et al., 2017) and references therein.

In this study we have applied LOTOS-EUROS version 2.2 with a total number of 12 vertical layers. The meteorological input is retrieved from the ECMWF 00.00 GMT and 12.00 GMT operational forecasts at ~9 × 9km resolution. The 12 levels are a combination of the first 33 hybrid levels from the meteorological input (3 × 1, 6 × 2 and 3 × 6 layers from surface to top). With this approach the vertical resolution gradually increases from ~20 m for the surface layer to ~2 km for the top 3 layers up to an altitude of ~8 km. We have used a nesting approach with two model runs. One run on a coarse domain (~20 × 20km) over Europe [−15.0W-35E; 35N–70N] and a zoom run over Germany and Poland [2E-16E; 47–56N] on a finer resolution of ~6 × 6km. The chemical boundary conditions for the European run are retrieved from the global C-IFS (Integrated Forecasting System including Chemistry) model system (Marécal et al., 2015).

For the emissions we have used the TNO 'science-based' emissions inventory (Denier Van Der Gon et al., 2015), which is an extension of the standard MACC/CAMS emission inventories developed by TNO (Kuenen et al., 2014, 2021). The extension incorporates an update of the residential wood combustion emissions, taking a consistent approach for all European countries, including condensable material.

As we have seen that the model has difficulty in reproducing high PM levels during cold and stable weather conditions, a couple of updates, in addition to the use of the updated residential wood combustion emissions, have been implemented. These are:

- An update of the deposition over snow. This results in lower deposition values over snow covered arable and grass land. In addition, below −5 °C, ice settings for deposition are applied to snow surfaces. The update leads to a small increase of PM concentrations in case of snow and cold temperatures.
- The use of the heating degree approach for residential combustion emissions. This approach uses the actual temperature to distribute the yearly total emissions over the days in the year. For daily averaged temperatures below 17 °C, it is assumed the heating demand increases, leading to higher emissions. In the approach 20% of the residential combustion emissions is still independent of temperature (these reflect for example cooking emissions). The heating degree approach can lead to a factor of 2 higher emissions from residential combustion during cold spells.
- The use of the multiple vertical layer option in the model as opposed to the original 5- dynamical layer version, which was known to overestimate the vertical mixing during stable weather conditions.

2.2. Source attribution in LOTOS-EUROS model

Within the FP7-project EnerGEO, a system to track the impact of emission categories within a LOTOS-EUROS simulation is developed. This system is based on a labelling technique (Kranenburg et al., 2013), which follows emitted components through the model system. With this technique, besides species concentrations, the contributions of pre-defined source categories are calculated. The labelling routine is implemented for primary, inert aerosol tracers as well as chemically active tracers containing a C, N (reduced and oxidized) or S atom, as these are conserved and traceable. The source apportionment module for LOTOS-EUROS provides a source attribution valid for current atmospheric conditions as all chemical conversions occur under the same oxidant levels. For details and validation of this source apportionment module we refer to (Kranenburg et al., 2013). The source apportionment technique has been previously used to investigate the origin of particulate matter (episodes) (Hendriks et al., 2013; Timmermans et al., 2017) and nitrogen dioxide (Schaap et al., 2013).

For secondary aerosols consisting of two components (e.g. ammonium nitrate (NH_4NO_3) half of the mass is attributed to the ammonium source sector or location (mostly ammonia (NH_3) from agricultural sources) and half of the mass to the nitrate source sector or location (a.o. nitrogen dioxide (NO_2) from traffic). Both components are required for formation of the combined aerosol. The contributions are preserved when transported to another region. The chosen method leads to a larger agricultural contribution than the method where the ammonium nitrate mass is allocated to the ammonium and nitrate sources based on the respective molecular masses of these components (NH_4^+ is lighter then NO_3^-). Because the combined aerosol cannot be formed if either of the two components is unavailable, attributing equal contributions seems justified.

2.3. Observations from PM-Ost campaign

Observational data is taken from the 'PM-Ost' campaign, conducted during winter 2016/17 at several sites in East Germany and reported in detail in van Pinxteren et al. (2019). Briefly, 24 h high-volume filter samples were taken on a daily basis from September 2016 to March 2017 at 6 rural background sites, 2 urban background site, and 2 urban traffic sites, which are given with their respective abbreviations in Table 1. Most stations belong to the air quality monitoring networks of the federal states, except for UBNEU, which is run by the German Environmental Agency Umweltbundesamt (UBA) and SNMEL, run by the Leibniz Institute for Tropospheric Research (TROPOS).

From these samples, concentrations of gravimetric PM10 mass, inorganic ions as well as organic and elemental carbon (OC/EC) were analysed or provided in the PM-Ost project. In addition, for 80 days selected as intensive measurement days with a focus on high pollution episodes, concentrations of polycyclic aromatic hydrocarbons (PAHs), and levoglucosan were determined at most sites. At the two Berlin sites, trace metal concentrations were determined for the intensive measurement days, which were not reported yet in van Pinxteren et al. (2019). These measurements were done using a total X-ray fluorescence spectroscopy method described by Fomba et al. (2018) and yielded concentrations of Ti, Mn, Fe, Ni, Cu, Zn, As, Se, Sr, Ba, and Pb.

2.4. Source attribution through PMF

Source apportionment was performed applying the positive matrix factorisation (PMF) receptor model with the EPA PMF version 5 software (US EPA, 2014), as detailed in van Pinxteren et al. (2019). Briefly, pooled data from all sites was used and different numbers of factors were tested and evaluated for plausibility. The final solution for all measurement days using PM10 mass, inorganic ions and OC/EC data resulted in 6 resolved factors, representing fresh salt (mainly sodium chloride), aged salt (mainly sodium nitrate/sulfate plus some OC), secondary I (mainly ammonium nitrate), secondary II (mainly ammonium sulfate and OC), combustion (mainly OC and some EC), and traffic (mainly OC, EC, nitrate and calcium). The final solution for the 80 selected days including levoglucosan concentrations resulted in a split of the original combustion factor into a general combustion and a biomass combustion factor, with the latter one being identified mainly by its high contribution of levoglucosan as a characteristic marker compound. These two PMF solutions were already reported and discussed in van Pinxteren et al. (2019) and their profiles are given in the supplemental material as Figs. S1 and S2. A third solution for the two Berlin sites and the selected 80 days was obtained in the project, but not reported earlier. The inclusion of trace metal concentrations allowed for discriminating traffic contributions into abrasion or wear particle mass, indicated by high contributions of Fe and Ba as typical tracers (Pinxteren et al., 2016), and resuspended crustal material with high contributions of calcium, sulfate, Ti, and Sr. In addition, a coal combustion factor, in addition to the general combustion and the biomass combustion factors could be resolved, mainly based on contributions of sulfate, As, and Pb, which have been used earlier already as coal combustion indicators

Table 1
Overview of PM-Ost stations, their type and location.

Federal state	Station	Station type	Abbreviation	Latitude	Longitude	Altitude (m)
Berlin	Frankfurter Allee	Traffic	BEFRA	52.514072	13.469931	40
	Nansenstr.	Urban	BENAN	52.489451	13.430844	35
Brandenburg	Potsdam	Traffic	BBPOT	52.393932	13.037474	31
	Hasenholz	Rural	BBHAS	52.563835	14.015252	88
	Cottbus	Urban	BBCOT	51.746344	14.33455	75
	Neuglobsow (UBA)	Rural	UBNEU	53.142367	13.03233	65
Mecklenburg-Western Pomerania	Löcknitz	Rural	MVLOE	53.520456	14.257407	17
Saxony	Brockau	Rural	SNBRO	50.608136	12.211112	430
	Niesky	Rural	SNNIE	51.285356	14.749731	148
	Melpitz (TROPOS)	Rural1	SNMEL	51.528177	12.938227	86

(Pinxteren et al., 2016). The factor profiles of the 9 source categories for the Berlin sites are given in the Supplement as well (Fig. S3).

3. Results & discussion

3.1. Evaluation modelled concentrations

The LOTOS-EUROS modelled concentrations have been evaluated through comparison with the observations from the PM-Ost campaign. In the evaluation we use the following metrics:

Mean bias: $Bias = \frac{1}{N}\sum (C_{model} - C_{observation})$

Root mean square error: $RMSE = \sqrt{\frac{1}{N}\sum (C_{model} - C_{observation})^2}$

Temporal correlation: $R^2 = \left(\frac{\sum (C_{model} - \overline{C_{model}})(C_{observation} - \overline{C_{observation}})}{\sqrt{\sum (C_{model} - \overline{C_{model}})^2 \sum (C_{observation} - \overline{C_{observation}})^2}} \right)^2$

Where C is the concentration from the model or observation and N is the number of values over which the mean is calculated.

In Fig. 1, the daily PM10 observations are compared to the modelled results for the station Melpitz (SNMEL). For September 2016, a systematic underestimation is observed. After September, the modelled PM10 levels nicely follow the observed variability, except for two episodes. The first period with enhanced concentrations missed by the model occurs around the 10th of November. Around this date observed concentrations are above 40 μg/m^3, where the model predicts less than half of these observed concentrations. The second episode missed occurs in the first half of February. During the second half of January and the first half of February 2017, values above the EU limit value of 50 μg/m^3 were observed. In general, the model result follows the observed daily pattern, but the largest episode peak in the beginning of February is not fully captured. During these days, the weather was characterized by easterly winds and particularly cold weather across central and eastern Europe. During such periods, the meteorological boundary mixing layer is shallow, allowing combination of local build-up and transboundary transport of air pollution. Such situations are typically difficult for the models to capture. The boundary layer height in LOTOS-EUROS comes from the meteorological input from the ECMWF IFS model. The IFS model associates the boundary mixing layer with a specific value of the bulk Richardson number (0.25) which characterises the degree of turbulence (ECMWF, 2021). There are some issues and uncertainties associated to this approach (Von Engeln and Teixeira, 2013) and although few evaluation studies exist, there are indications that low boundary layer heights are overestimated (Seidel et al., 2012; Uzan

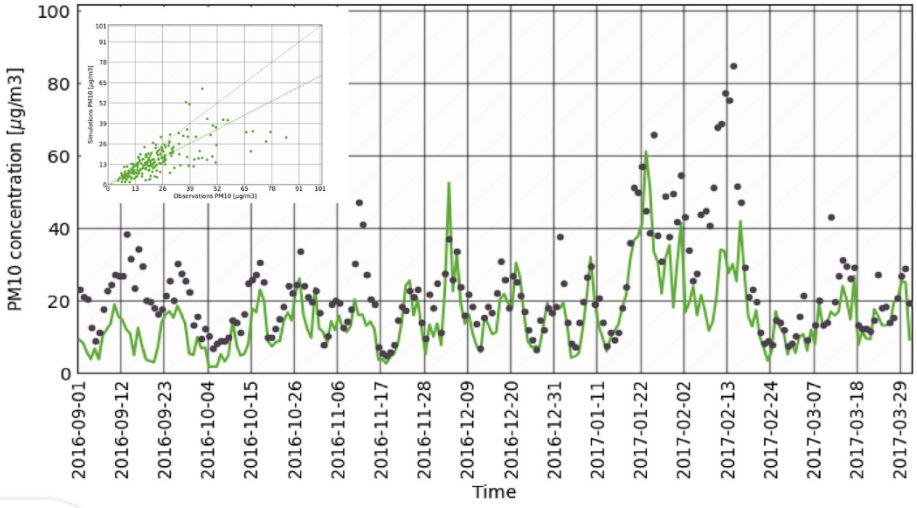

observed daily PM10 in Melpitz. Inset shows scatterplot between modelled and observed daily PM10 concentrations.

Table 2
Metrics of model comparison with observations for PM-Ost campaign.

Station	Bias	Correlation (R^2)	RMSE
BEFRA	−14.44	0.27	23.25
BBPOT	−12.80	0.41	17.52
BENAN	−7.96	0.34	14.60
BBCOT	−9.08	0.52	14.09
BBHAS	−7.40	0.44	12.42
MVLOE	−9.01	0.63	14.79
UBNEU	−4.63	0.46	9.37
SNBRO	1.19	0.50	7.64
SNNIE	−4.09	0.54	11.10
SNMEL	−7.63	0.51	12.46

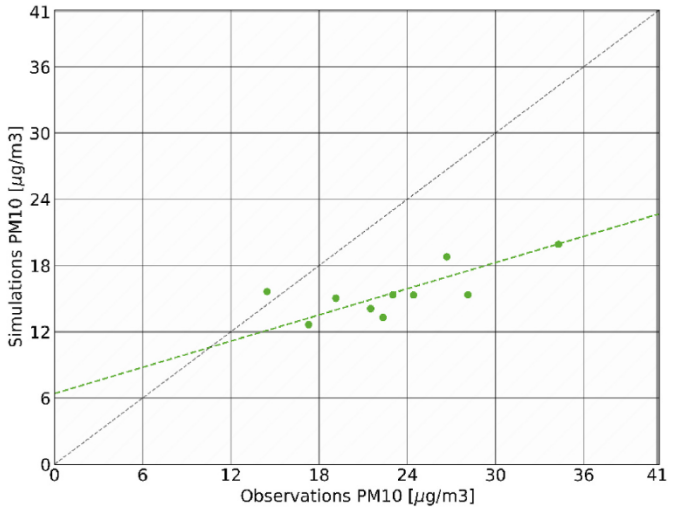

Fig. 2. Modelled and observed winter 2016/2017 mean PM10 concentrations for 10 stations in PM-Ost campaign.

et al., 2020).

All other stations in this study show similar modelled and observed temporal patterns as the station in Melpitz, including the high pollution episode in February. The temporal correlation is ranging between 0.27 and 0.63 with lowest correlations at the two Berlin stations (Table 2). A general underestimation around 30% is found (Fig. 2), with only one station showing overestimation by the model. This indicates that the model underestimation is not a local effect in Melpitz, but a larger scale issue over the whole domain, which will be discussed further in sections 3.4 and 3.5.

The comparison is influenced by a representativity issue for several sites. The single station showing an overestimation by the model is the station in Brockau. The elevated location of this station at a mountain range on the border between Germany and Czech Republic is expected to lead to a certain decoupling of the concentrations from those in lower-lying areas of the rural background, which is difficult to capture by the model. The largest bias and RMSE are found for stations in Berlin-Frankfurter Allee (BEFFA) and Potsdam (BBPOT), which are both traffic stations. At those stations, a large local contribution from traffic influences the observed levels, which cannot be captured by the model because of the fact that the traffic emissions are instantly mixed into the relative coarse model grid cells of $6 \times 6 km^2$. For other stations, we found smaller biases and RMSE values, see Table 2. Note that these stations were included in the comparison as they can provide valuable information on the non-traffic sources.

To further illustrate the model performance for PM10 we present the comparison for individual PM components for Melpitz in Fig. 3. Here we see that an underestimation of observed levels of OC is present while EC [illegible] concentrations from end of November [illegible] produced, but the observations are largely underestimated during the episode in February 2017. Another component which is underestimated by the model during the February episode is sulfate (see bottom plot Fig. 3). This underestimation of sulfate is a common feature for regional air quality models in different parts of the world (Fagerli and Basart, 2021; Tuccella et al., 2012; Wang et al., 2014). The different behavior of the components indicates that there is no single explanation for the differences between modelled and observed concentrations.

The individual components and the underestimations in each do not add up to the total observed PM mass and its underestimation, indicating that other components are present which are also underestimated.

The comparison of the source apportionment results with the PMF results in section 3.4 will provide hints to further identify the missing modelled mass and underestimated sources. Possible missing components will be discussed in section 4.

3.2. Source attribution by LOTOS-EUROS

In this section we present modelled dominant country and source sector contributions to the PM10 concentrations in Eastern Germany for our study period. We start with a presentation of the regional origin of the modelled PM10 concentration contributions to investigate the origin of the air masses during the elevated PM10 concentration episodes in January–February. Fig. 4 (top plot) shows the timeseries of modelled PM10 concentration at the station of Melpitz and the modelled contributions from Germany, Poland, other countries and the boundaries of the model domain. The region of origin changes from day to day and may differ in the different stages of a period with limit values exceedances. Substantial contributions from Poland and other countries outside Germany are found, especially in the February episode where the national contribution is minor. During this event the contribution from the countries further South or East of Poland are as important as the Polish contributions. The same characteristic is noted for the missed episode at the beginning of November, whereas the captured patterns with enhanced concentrations have a more domestic signature.

In Fig. 4 (bottom plot), the timeseries of modelled PM10 concentration, at the station of Melpitz, is shown including modelled contributions from different emission sectors. The largest contribution during the January–February winter episodes is from residential combustion (light blue). The time series illustrates the large seasonal variation in the relevance of residential combustion as its contribution is hardly present in the modelled time series in September. Also, the energy sector contributes variably, as its contribution is clearly larger during periods with air masses arriving from eastern Europe. Outside the high pollution events in January–February, contributions are more equally divided over other sectors with significant contribution from agriculture, due to the formation of ammonium nitrate.

Average source contributions for all stations are shown in Fig. 5 (top plot). As presented in the previous section the model is underestimating the observed PM10 concentrations during the study period. Following (Hendriks et al., 2013) we therefore introduce a contribution of the non-modelled mass and present the modelled source contributions relative to the observed concentrations. The non-modelled mass is determined as the observed concentrations minus the modelled value and encompasses all model errors, including non-modelled source contributions such as road salting and Secondary Organic Aerosol (SOA) and the net result of under- and overestimations of included source contributions. All stations show a similar source attribution as seen at Melpitz, with a larger share of non-modelled mass at both traffic stations (BEFRA and BBPOT). Residential combustion and agriculture are the most important sources, with an average share of around 29% and 17% for the modelled mass respectively, which translates to 19 and 12% of the observed mass.

For Melpitz a more detailed source contribution is shown in Fig. 5 (bottom plot) where all source contributions are presented for different pollution levels. For each measured bin of 5 $\mu g/m^3$ of PM10 the average

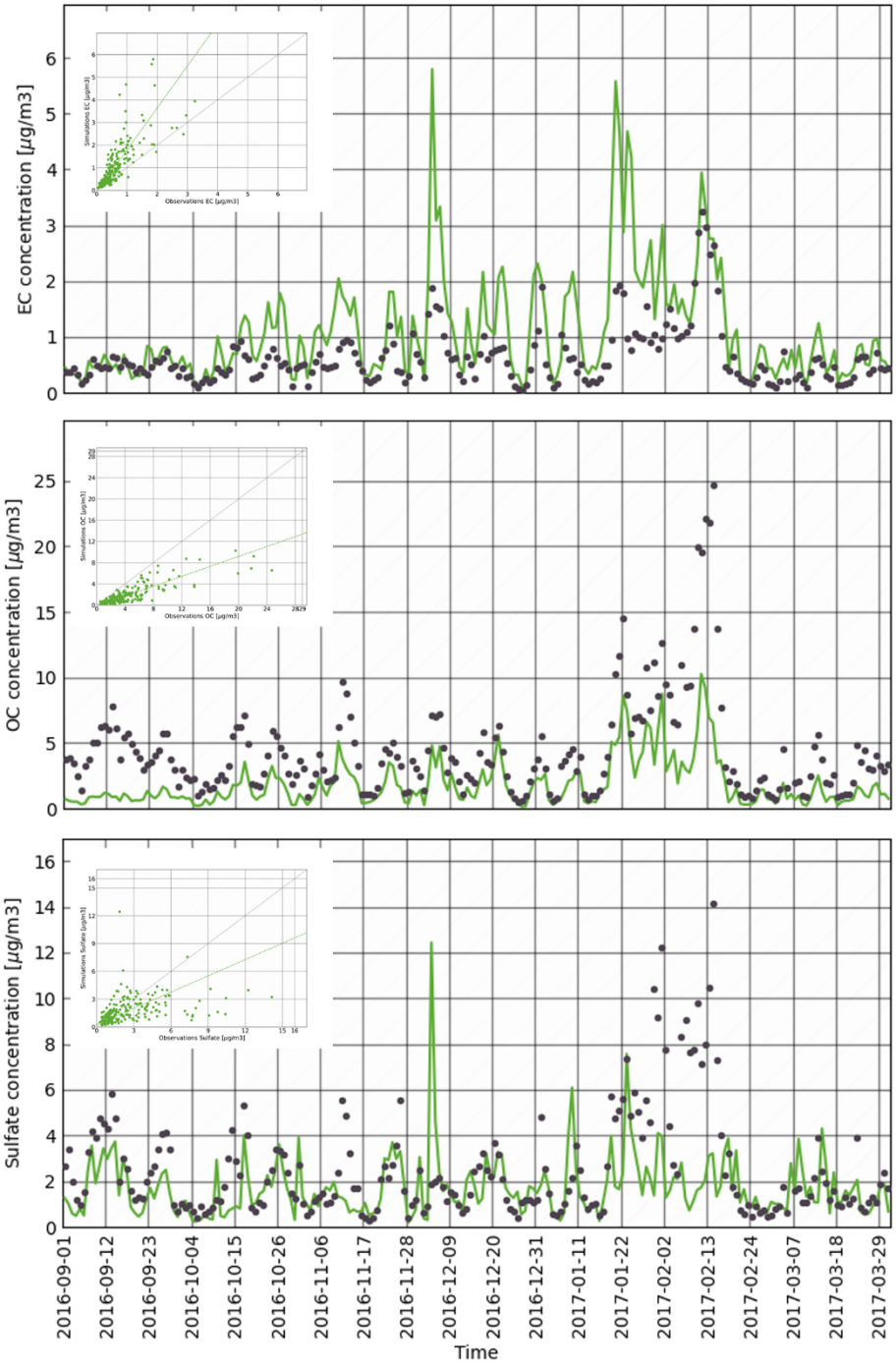

Fig. 3. Modelled daily EC, OC and SO_4^{2-} concentrations (green line) compared to observed values at the station of Melpitz. Inset shows scatterplot between modelled and observed daily concentrations. (For interpretation of the references to colour in this figure legend, the reader is referred to the Web version of this article.)

source contribution over the whole study period is shown. In Table 3 this is summarised for 3 size bins.

Low concentrations during wintertime usually coincide with higher windspeeds and unstable conditions with higher temperatures. This is also represented in the source contributions for the low concentration levels below 15 µg/m^3, where the contributions of natural sources (sea salt and Saharan dust) are relatively large. At higher concentrations the two most important sources are residential combustion and agriculture. Smaller contributions are visible from power plants, industry and transport (road and non-road). The share of modelled values attributed to residential combustion increases for the highest concentration bins [illegible] observed values decreases). This is related to the link between high PM10 concentrations and cold temperatures. During winter the residential heating emissions rise, increasing its contribution to the total PM10 concentrations.

3.3. Source attribution by PMF

The results from the source attribution of PM10 by PMF are presented in van Pinxteren et al. (2019). They found average traffic contributions of 30% at the traffic station in Berlin (BEFRA) and 15% at urban background stations. The contributions from combustion ranged between 20 and 30%, from secondary formation of ammonium sulfate and organics between 20 and 40%, from the formation of ammonium

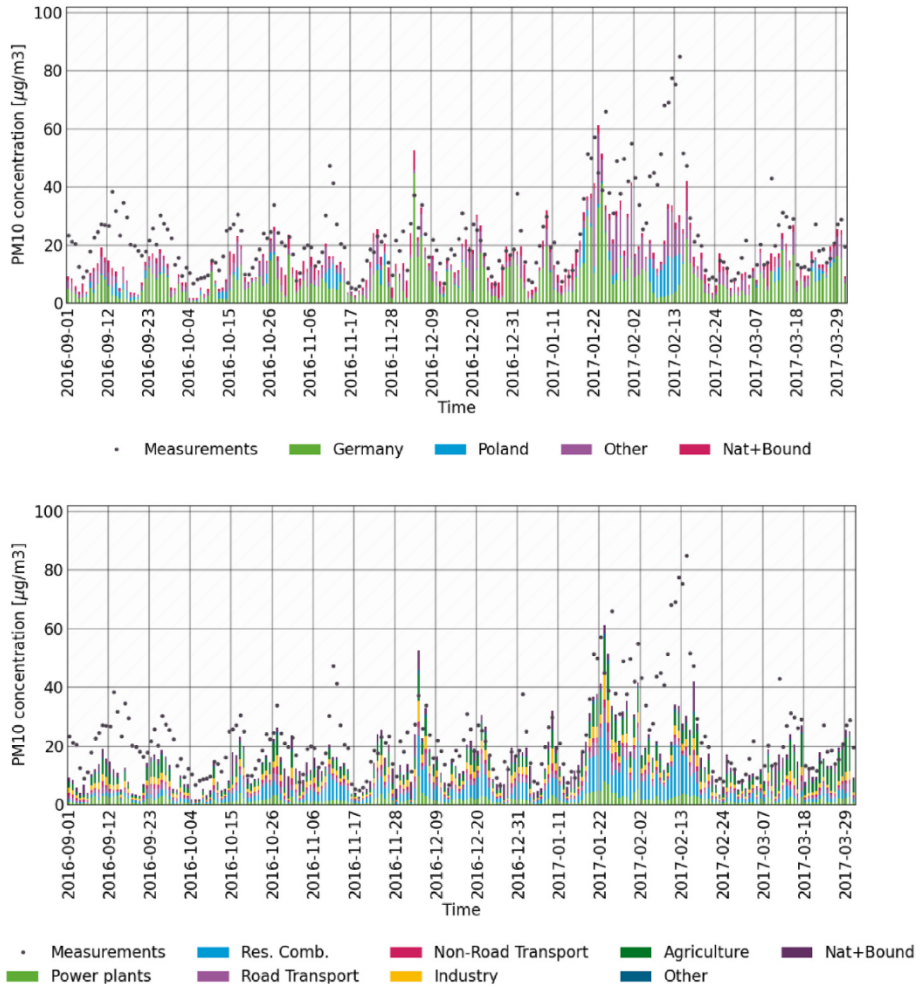

Fig. 4. Timeseries of daily PM10 mass at Melpitz, regional contributions from different regions (top plot, Germany, Poland and other countries) and contributions from different source sectors (bottom plot).

nitrate between 15 and 30% and from fresh and aged salt around 10%. When focusing on pollution episodes with increased PM10 concentrations, observed during 80 intensive measurement days, most of the relative contributions did not change very much. However, the split between 'other' combustion and biomass combustion contributions available for these intensive measurement days, showed a dominant contribution from the latter indicating that wood combustion (and potentially also lignite combustion contained within the biomass combustion factor) were important sources of PM10 for the studied period and sites.

3.4. Comparison of both methods

To evaluate the performance of the tagging source attribution within LOTOS-EUROS, the results are compared to the results from the receptor-based attribution achieved with the PMF method applied to the PM-Ost campaign data. It should be noted here that the source categories contained in the various approaches are not always completely identical. Table 4 describes the source categories that are compared between the two models, as well as their determination from the model data. The comparison is limited to anthropogenic source categories for which the individual components and sectors contained in LOTOS-EUROS can be meaningfully combined to map the source categories determined in the PMF as well as possible.

natural salt factor is not given here, but
ibutions determined by PMF (sum of fresh and aged salt, 2.1–2.9 µg/m^3 in the rural background) are higher than the sea salt contributions calculated in LOTOS-EUROS, which were determined from oceanic sodium multiplied by 3.6 as the conversion factor from sodium to total sea salt and were 1–1.9 µg/m^3 at the rural background stations (Fig. S4). This difference is presumably due to the mass contributions of nitrate, sulfate and partly also organic material contained in the PMF factor "aged salt", which are not included in the LOTOS-EUROS source contributions. This is supported by the comparison for the category ammonium nitrate (Fig. S5), where the PMF contributions at the rural background stations are up to 2 µg/m^3 lower than the LOTOS-EUROS contributions.

General traffic contributions were determined with PMF for all days and stations. For the two Berlin measuring stations for which trace metal concentrations were available for 80 selected measuring days a distinction was made between emissions caused by the resuspension of road dust and abrasion of brakes and tires. In Fig. 6, the total PMF traffic contributions are compared with the total PM mass from the LOTOS-EUROS sector "road traffic".

It can be clearly seen that the PMF at the city stations and here in particular at the BEFRA traffic station produces traffic source contributions higher by a factor of 2–5 than calculated by LOTOS-EUROS. This is due to local, small-scale contributions that cannot be resolved by the LOTOS-EUROS model. In the rural background, the PMF traffic contributions are still somewhat higher, but with mostly 1.5–2.0 µg/m^3 (except MVLOE) they are closer to the LOTOS-EUROS contributions of 1–1.6 µg/m^3.

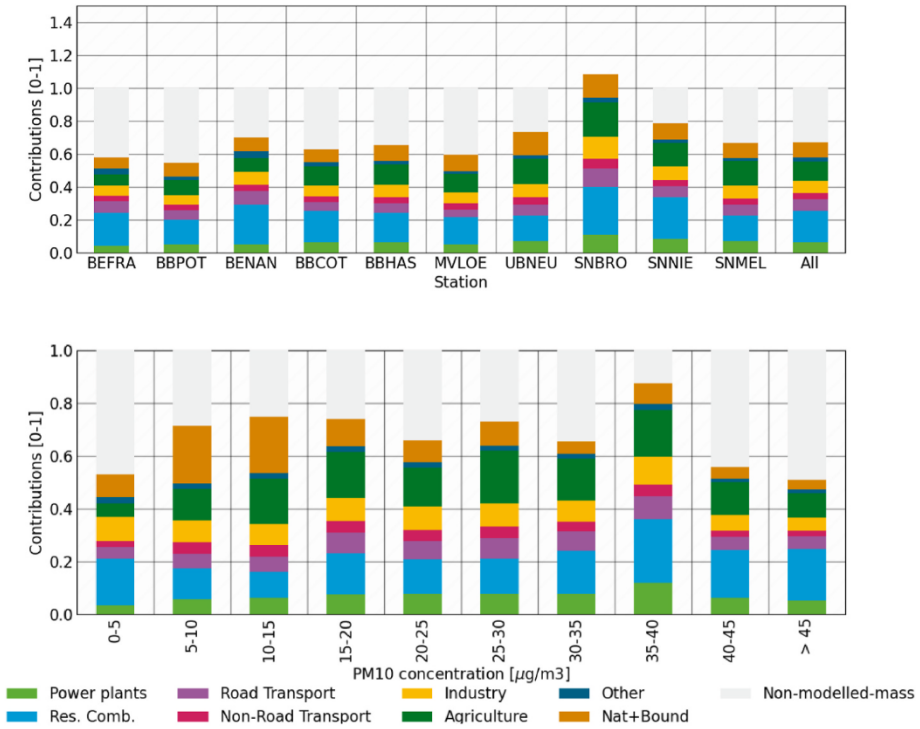

Fig. 5. Average source contributions to PM10 at all stations (top plot) and source contributions for PM10 in Melpitz divided by pollution level (bottom plot).

Table 3
Average relative source sector contributions (in %) to PM10 in Melpitz for 3 size bins.

Sector	Concentration bins (in µg/m^3)			All
	0–15	15–30	>30	
Power plants	6.0	7.7	6.8	7.1
Residential Combustion	10.5	13.9	19.3	15.5
Road Transport	5.7	7.6	5.9	6.6
Non-Road Transport	4.4	4.4	2.7	3.7
Industry	8.2	8.8	6.4	7.8
Agriculture	15.4	17.4	12.3	15.1
Other	2.0	2.0	1.6	1.8
Natural + Boundaries	21.5	9.2	4.6	9.2
Non-modelled mass	26.3	29.2	40.4	33.1
Number of observations per bin	67	102	42	211

The increased PMF traffic contributions observed at many stations, especially at the beginning of the measurement period, could indicate contributions from the resuspension of crustal material, which, due to their chemical similarity to resuspended road dust, may be mixed into the PMF traffic factor to a certain extent. The similar magnitude of the traffic contributions in the rural background in both models suggests, however, that a large part of the source contributions is actually due to background pollution from traffic emissions.

The lack of correlation of the model values at all stations suggests that the either very local (BEFRA) or diffuse (in the background) source category traffic (total exhaust gas, brake and tire wear and resuspension) is difficult to be modelled in a time-consistent manner with the two approaches used here.

Several studies (e.g. Suarez-Bertoa and Astorga, 2018; Weilenmann et al., 2009) show that traffic exhaust emissions increase during periods with low temperatures related to extra emissions from cold starts and inefficient engine modes. For example, a compilation of on-road remote sensing shows that EURO-5 diesel cars emit 50% higher NOx at 10 °C than at around 20 °C (Borken-Kleefeld et al., 2018). In our experiment [illegible] average traffic intensity patterns and have no dependence on temperature.

The reasons for the sometimes very high deviations observed in cities close to the source are partly caused by non-exhaust emissions. Indeed, the contribution for resuspension at the urban background BENAN station as determined with the PMF is considerable with 5.5 µg/m^3 (not shown here). In the model run performed in this study this contribution is not included. The contribution of the other non-exhaust emission source 'brake and tire wear' (Fig. S6) is smaller (0.4 vs. 0.8 µg/m^3 for PMF and LOTOS-EUROS, respectively). It should be taken into account that due to the lack of specific tracers, the PMF could not resolve the PM source contributions from direct engine emissions which are probably mixed in with both non-exhaust-traffic factors. The actual difference to the LOTOS-EUROS contributions should therefore be slightly smaller.

The comparison for the category combustion is presented in Fig. 7. Source contributions from all combustion emissions were determined by PMF for all days and for the selected measurement days a distinction could be made between "biomass combustion" and "other combustion". The distinction was possible due to the available concentrations of levoglucosan as a characteristic ingredient of PM emissions from wood combustion. Note that there are indications that emissions from lignite combustion can also contain significant levels of levoglucosan (Fabbri et al., 2009; Yan et al., 2018). Hence, an unspecified share of the PMF source category "biomass combustion" may thus also reflect the contribution of this fossil fuel, which is still used extensively in some Eastern European countries. For the Berlin sites and selected days, based on arsenic as a coal tracer, coal combustion was also identified as a further source category. The LOTOS-EUROS source contributions were calculated as shown in Table 4 from the PM10 total mass of the sectors of energy generation from biomass and coal, as well as residential combustion, i.e. building heating with coal and biomass.

At almost all stations, there is good agreement between the combustion contributions calculated with both models. This applies both to the amount of the contributions, which averaged between 3.3 and 7.2 µg/m^3 for LOTOS-EUROS and between 3.3 and 7.7 µg/m^3 for PMF, as well as for their temporal correlation with R^2 mostly between 0.4 and 0.64. The somewhat poorer correlation in Berlin (R^2 = 0.3–0.35) is due to a period at the beginning of January during which the LOTOS-EUROS

e 4
ce categories used for the source contribution comparisons.

rce category	PMF Factor	PMF Data availability	LOTOS-EUROS Components	LOTOS-EUROS Source Sector
monium nitrate	Secondary I (AN)	all Days, all Stations	Nitrate x 1.29	Total from all sectors
ffic	Traffic	all Days, all Stations	Total mass	Road traffic
ffic (Resuspension)	Traffic (Resuspension)	Selected days, Berlin stations only	Dust	Road Traffic
ffic (Brake and Tire wear)	Traffic (Brake and Tire wear)	Selected days, Berlin stations only	Other PM	Road Traffic
ombustion	Combustion	all Days, all Stations	Total mass	Energy (Coal) + Residential combustion (Coal) + Energy (Biomass) + Residential combustion (Biomass)
Combustion (Biomass)	Combustion (Biomass)	Selected days, All stations	Total mass	Energy (Biomass) + Residential combustion (Biomass)
Combustion (Coal)	Combustion (Coal)	Selected days, Berlin station only	Total mass	Energy (Coal) + Residential combustion (Coal)

source contributions were significantly higher than those of the PMF. A possible cause could be an error in the spatial distribution of emissions. It is expected that the share of residential wood combustion in large cities is small, however the emission inventory positions a relatively large contribution of these emissions in the cities due to the proxies used for the distribution over the country. An experiment with an adapted distribution where emissions are partly moved from the city centres to less densely populated areas in the outskirts of the cities, with buildings that mostly have their own combustion system, showed a clear improvement in the performance of the LOTOS-EUROS model for black carbon in Berlin and the east of Germany (Manders et al., 2021).

The spatial variability of the mean combustion contributions also agrees quite well, with the largest values in Berlin and the lowest contributions in UBNEU. A comparably larger difference is seen for BBCOT. In Cottbus (BBCOT), the mean source contribution according to PMF is similar to that in Berlin and according to LOTOS-EUROS is closer to that in the rural background, which may be related to local emissions.

The picture for biomass combustion (Fig. S7) is very similar to the overall combustion category. For the contributions and their temporal and station-dependent trends, the same findings can be found for the 80 special measurement days as discussed above for all measurement days, which is due to the fact that the total combustion emissions in both models are dominated by biomass combustion emissions.

Alternatively, the comparison for coal combustion for Berlin nicely illustrates the challenge for sources with a large contribution to secondary particulate matter. If we compare the PMF coal combustion contribution to the LOTOS-EUROS coal combustion contributions without the contributions from the secondary inorganic aerosols (ammonium, sulfate and nitrate) (Fig. S8), they are very similar for the two Berlin sites with values of 0.8 μg/m^3 from PMF and 1.1–1.3 μg/m^3 from LOTOS-EUROS.

If we also in the LOTOS-EUROS coal combustion part add the contribution from the secondary inorganic aerosols which result from SO_2 and NO_x emissions, the values are approximately doubled (Fig. S9). In this case the PMF values are about 3 times lower at both stations and the R^2 is low around 0.2. Because the PMF coal combustion factor is heavily based on the variability of arsenic as a coal tracer it mainly represents primary coal emissions. Additionally, arsenic possibly does not very well represent the emissions from coal combustion of various sources.

Overall, it can be concluded for the source category combustion that both models describe the source contributions, especially for total combustion and biomass combustion, in good agreement despite their very different approaches, which increases confidence in the values determined for the study area.

3.5. Evaluation of non-modelled mass

As presented in section 3.1, when comparing the total PM10 mass concentration modelled by LOTOS-EUROS at the stations of the PM-Ost project with the measured concentrations, there is a part of the observed PM10 concentration that is not explained by the chemical transport model. Fig. 8A and B shows the concentration time series and average values of this so-called non-modelled mass at all stations. To obtain information on possible source categories that could be the cause for this, the non-modelled mass was subjected to a correlation analysis with the PMF source contributions.

Fig. 8C shows the Pearson correlation coefficients for the BEFRA traffic station where, as explained and expected, the highest non-modelled mass concentrations occurred. Significant correlations with $r = 0.55$ and 0.52 are found for the source categories secondary ammonium sulfate and organic material and traffic, respectively, while further correlations with $r = 0.46$ and 0.38 were found for combustion and fresh salt, respectively. As described above, the very local traffic emissions at BEFRA cannot be represented sufficiently well due to the resolution of the LOTOS-EUROS model and are one of the main reasons

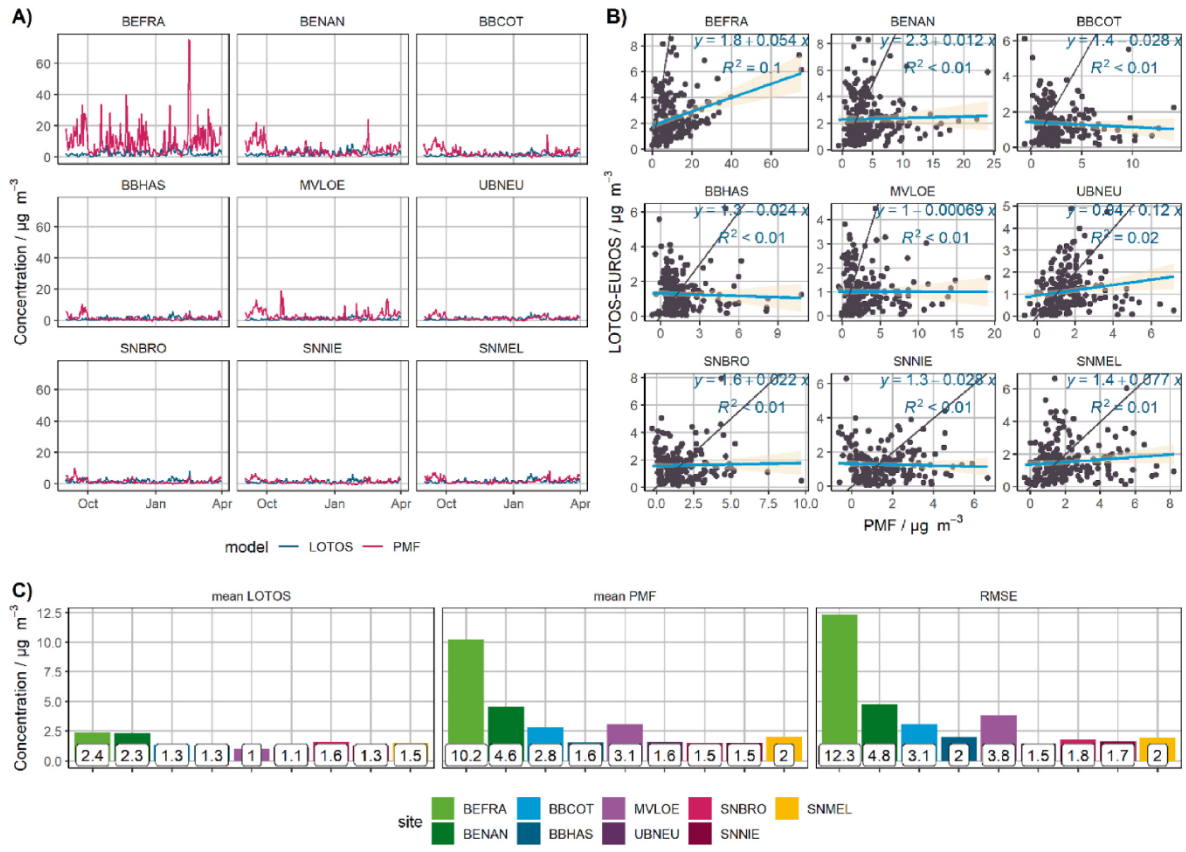

Fig. 6. Comparison between LOTOS-EUROS source contributions and PMF for traffic. A) Time series of source contributions, B) scatter plots of source contributions, and C) mean source contributions and RMSE between both approaches.

for the large difference between the measured and modelled mass concentration at this station. The source category fresh salt fits in with this, as it mainly represents road salt emissions at BEFRA, which also occur locally. The correlations with the source categories secondary II (AS+OC) and combustion indicate another main cause of non-modelled mass, which is also observed at rural background sites and discussed in the following.

Fig. 8D shows the correlation coefficients between non-modelled mass and PMF source contributions at the rural background stations, whereby the station SNBRO was not taken into account here due its atypical deviation described above. A very high correlation coefficient of the non-modelled mass ($r = 0.77$) is found with source contributions from secondary II factor, i.e. ammonium sulfate and organic material, and further, with $r = 0.59$ and $r = 0.48$, strong but somewhat weaker correlations are found with combustion and ammonium nitrate, respectively. It should be noted that the PMF source contributions of these 3 source categories are correlated with each other with r between 0.47 and 0.58, since gaseous combustion emissions such as NO_x, SO_2 and volatile organic compounds (VOC) can produce secondary particulate matter in the form of ammonium nitrate, ammonium sulfate and organic material, during the chemical aging in the atmosphere. The high correlation coefficient with the secondary II category (AS + OC) is consistent with the underestimation of sulfate levels (see Fig. 3). Furthermore, it suggests that another main cause of the non-modelled mass might be the secondary formation of organic particulate matter (SOA) from VOC precursors, which is not implemented in the model version used in this study, but typically makes a significant contribution to the total PM concentration. The combustion of solid fuels, especially wood, but also coal, emits a large amount of VOCs (e.g. Bruns et al., 2016). Their conversion into SOA is a very complex but important process that is [illegible] ntal conditions. The process is complex to describe with a model but is especially important after transport and aging of air masses. The above-described good agreement between combustion source contributions from both modelling approaches reflects that the PMF combustion factor represents primary emissions mainly, including quickly condensable vapours similar to what is included in the LOTOS-EUROS emission inventories, while secondary processing during transport and aging is mainly part of the PMF secondary II factor. Under this assumption the high correlation of non-modelled mass with this factor as well as with the combustion factor would suggest that at least a part of the missing mass in LOTOS-EUROS is related to transformation of volatile combustion emissions, likely from solid fuels, to secondary particle mass. The contribution from SOA in this winter period and region is expected to be in the order a few µg/m^3 based on literature (Bessagnet et al., 2009; Ciarelli et al., 2017) and could therefore explain part of the underestimation. Ciarelli et al. (2017) showed observed wintertime (2009) SOA concentrations in Europe ranging between 0.4 and 4.4 µg/m^3 (1.2 µg/m^3 for Melpitz). Highest values were found in forest areas and southern sites.

4. Discussion

Our study is one of the first to compare source attribution from a tagging approach within a chemistry transport model to observational based source attribution using PMF. A relevant question is whether the calculated relative source contributions by LOTOS-EUROS are impacted by the model's underestimation. The comparison with the measurement-based source allocation using PMF provides us with some relevant information.

The comparison provides confidence in the combustion contribution determined for the study area by both methods, albeit that this contribution determined by the PMF method is probably mainly

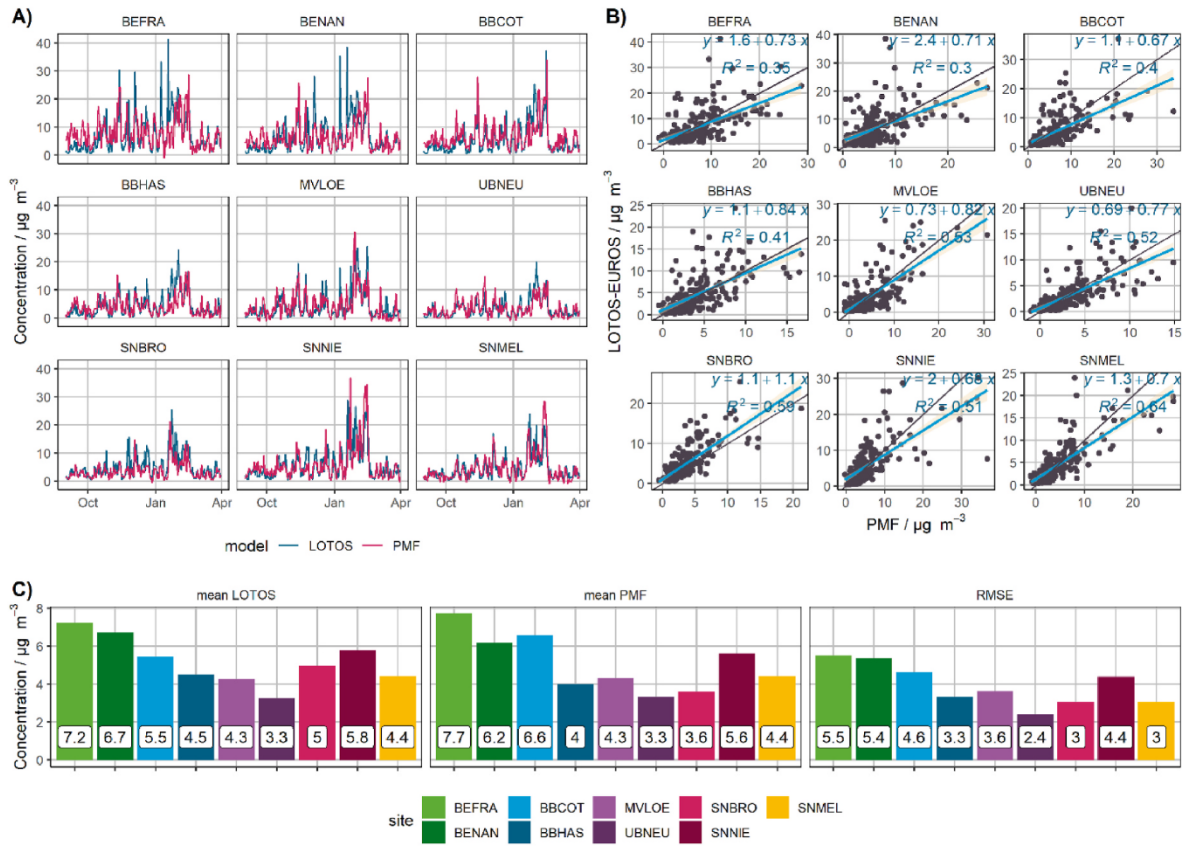

Fig. 7. Comparison between LOTOS-EUROS source contributions and PMF for combustion. A) Time series of source contributions, B) scatter plots of source contributions, and C) mean source contributions and RMSE between both approaches.

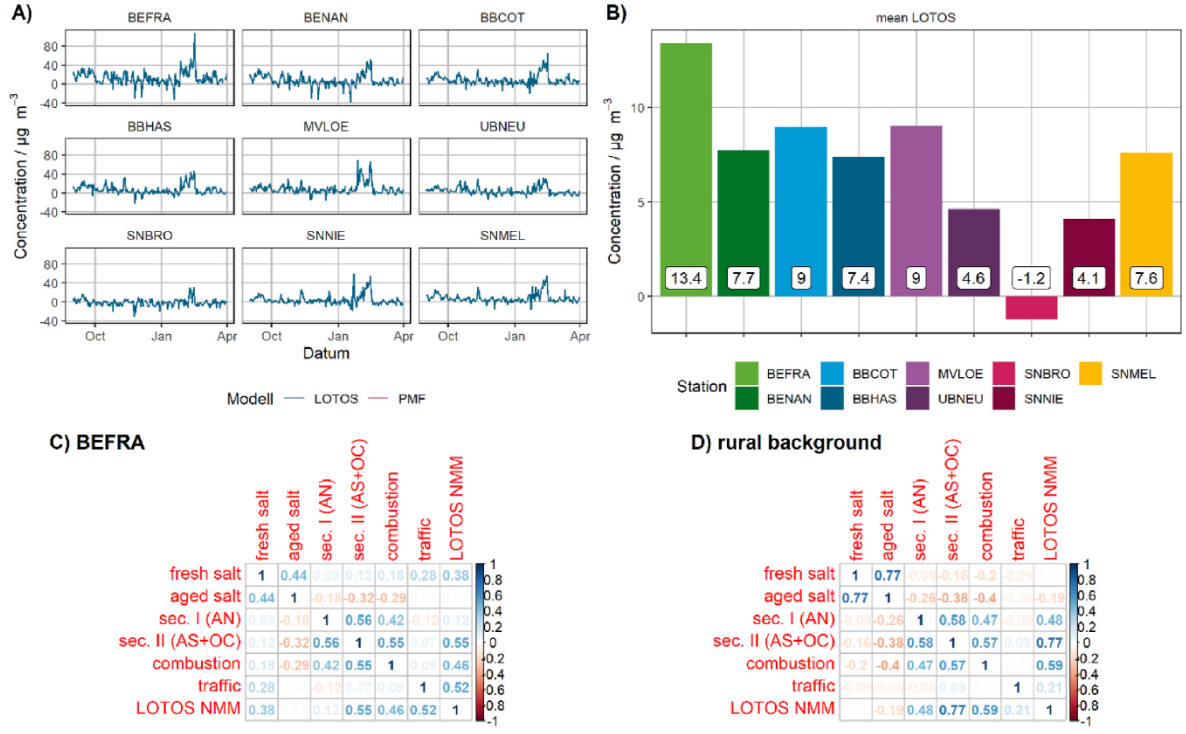

Fig. 8. A) Concentration time series of the non-modelled mass (, i.e. the difference between the measured PM10 concentration and the PM10 concentration modelled with LOTOS-EUROS) at all stations, B) mean non-modelled mass in the investigation period per station, C) Pearson's correlation coefficients of the non-modelled at the BEFRA traffic station, D) Pearson's correlation coefficients of the non-modelled Mass with PMF source contributions ut SNBRO).

representative for the primary emissions as discussed above in section 3.5 and the combustion contribution determined by the LOTOS-EUROS tagging method for primary emissions and the secondary inorganic aerosols. For the first time we used the PMF results to investigate the potential reasons for the underestimation of the total observed PM mass concentration. The high correlation of the non-modelled mass by LOTOS-EUROS with the PMF source contributions from ammonium sulfate and organic material suggests that to obtain the total contribution from combustion the LOTOS-EUROS model would need to implement secondary formation of organic particulate matter (SOA) from VOC precursors, for example using a volatility basis set (VBS) approach. In addition, we showed that sulfate is also underestimated by the model during the February episode (Fig. 3). Previous evaluations have also shown significant underestimation of sulfate during wintertime episodes (e.g. Banzhaf et al., 2015). Recently, the accelerated formation of SO_4^{2-} during severe pollution episodes has been discussed in several studies, proposing potentially important contributions from aerosol related heterogeneous and aqueous phase reactions (Harris et al., 2013; He et al., 2014; Wang et al., 2020, 2021) which are not represented in the model.

The contributions of the road transport emissions show a low correlation between the results of PMF and LOTOS-EUROS tagging. In addition, the concentrations assigned to traffic emissions are much higher for the PMF model than in the LOTOS-EUROS model. This can be partly explained by the absence of resuspension of road dust in LOTOS-EUROS. The inclusion of traffic resuspension is however far from trivial as empirical emission factors show a wide range in values (Amato et al., 2014, 2016). Furthermore, the emissions are likely to fluctuate depending on meteorological conditions (Amato et al., 2014). Another relevant aspect could be the variability in traffic exhaust emissions with ambient temperatures (Borken-Kleefeld et al., 2018; Suarez-Bertoa and Astorga, 2018; Weilenmann et al., 2009). The current (static) time profiles are based on mean traffic flow variability without any dependency on meteorological conditions for activities or emission factors. To address this issue the development of a dynamic approach for the temporal distribution of traffic exhaust emissions is planned.

Besides secondary organic aerosols and road dust resuspension there are other sources of PM missing in the model, such as road salting. During snowy conditions salt or sand is applied to roads to avoid slippery surfaces, these particles can become airborne from the traffic on the roads (Kolesar et al., 2018). This process is not included in the model and could be relevant during this specific episode with snow conditions. In addition, the aerosol water content could be a reason for the modelled underestimations (Tsyro, 2005). The observed concentrations are derived at 20 °C and 50% relative humidity. Under these conditions the aerosols contain water which contributes to the observed mass. This aerosol water content is not included in the modelled PM10 values presented here. For Melpitz during the January–February episode the aerosol water content can be calculated to reach values up to 12 μg/m^3. Considering the observed peak concentrations of 60–80 μg/m^3 in Melpitz this agrees with typical aerosol water content levels derived from filter weighing in lab conditions of 10–20% (Neusüß et al., 2002).

An ongoing comparison between modelled and observation-based source apportionment for French sites highlighted the role of organic matter in the form of biological material, such as fungal spores and plant debris. The empirical source apportionment based on a host of organic tracers show that primary biological material may contribute about 20% to annual average OC levels (Waked et al., 2014). These contributions peak during the growing season (Samaké et al., 2019) and therefore are not expected to be large during the January–February episode, but could be relevant for the PM10 concentrations in September which were also underestimated by LOTOS-EUROS.

Finally the PM10 episodes could have been impacted by desert dust. Analysis of global model data which are combined with satellite ob- sis data, available from the atmospheric opernicus.eu/ and MERRA model-2 data visible through https://giovanni.gsfc.nasa.gov/) indeed show some dust plumes reaching Germany in February, with peak dust values on the 16th of February. Indeed towards the end of the February episode (~16th of February) the contribution in the model from natural sources or boundaries is largest (bottom plot of Fig. 5). It could be possible that during the PM10 event, the model underestimates the dust concentrations.

Overall, this intercomparison study provided novel insights into the uncertainties associated with the source attribution of PM with a CTM (in this case LOTOS-EUROS) and ways to improve the performance. After implementation of stepwise improvements, a new comparison should be carried out to check whether this decreases the gap with observed PM concentrations during high PM pollution episodes and improves the agreement with the PMF source contributions. An expansion to other geographical areas (in Europe) may facilitate the evaluation of additional source sectors.

CRediT authorship contribution statement

R. Timmermans: Investigation, Supervision, Writing – original draft, Writing – review & editing. **D. van Pinxteren:** Conceptualization, Investigation, Formal analysis, Visualization, Writing – original draft, Writing – review & editing. **R. Kranenburg:** Methodology, Validation, Formal analysis, Visualization, Writing – original draft. **C. Hendriks:** Investigation, Validation, Formal analysis. **K.W. Fomba:** Formal analysis, Visualization, Writing – review & editing. **H. Herrmann:** Conceptualization, Supervision, Writing – review & editing. **M. Schaap:** Conceptualization, Supervision, Writing – original draft, Writing – review & editing.

Declaration of competing interest

The authors declare that they have no known competing financial interests or personal relationships that could have appeared to influence the work reported in this paper.

Acknowledgements

This work was supported by the German Environment Agency (UBA) in Dessau-Roßlau, through the FKZ 3716 51 203 0 project.

Funding for the PM-Ost measurement campaign is acknowledged from the Berlin Senate Department for the Environment, Transport and Climate Protection in Berlin, the Saxon State Office for Environment, Agriculture and Geology (LfULG) in Dresden-Pillnitz, the State Office for the Environment (LfU) of the Federal State of Brandenburg in Potsdam, and the State Office for Environment, Nature and Geology (LUNG) of the Federal State of Mecklenburg-Western Pomerania in Güstrow. Data provision is also acknowledged from the German Environment Agency (UBA) in Dessau-Roßlau.

Appendix A. Supplementary data

Supplementary data to this article can be found online at https://doi.org/10.1016/j.aeaoa.2022.100173.

References

Amann, M., Bertok, I., Borken-Kleefeld, J., Cofala, J., Heyes, C., Höglund-Isaksson, L., Klimont, Z., Nguyen, B., Posch, M., Rafaj, P., Sandler, R., Schöpp, W., Wagner, F., Winiwarter, W., 2011. Cost-effective control of air quality and greenhouse gases in Europe: modeling and policy applications. Environ. Model. Software 26, 1489–1501. https://doi.org/10.1016/j.envsoft.2011.07.012.

Amato, F., Cassee, F.R., Denier van der Gon, H.A.C., Gehrig, R., Gustafsson, M., Hafner, W., Harrison, R.M., Jozwicka, M., Kelly, F.J., Moreno, T., Prevot, A.S.H., Schaap, M., Sunyer, J., Querol, X., 2014. Urban air quality: the challenge of traffic non-exhaust emissions. J. Hazard Mater. 275, 31–36. https://doi.org/10.1016/j.jhazmat.2014.04.053.

Amato, F., Zandveld, P., Keuken, M., Jonkers, S., Querol, X., Reche, C., Denier van der Gon, H.A.C., Schaap, M., 2016. Improving the modeling of road dust levels for Barcelona at urban scale and street level. Atmos. Environ. 125, 231–242. https://doi.org/10.1016/j.atmosenv.2015.10.078.

Banzhaf, S., Schaap, M., Kerschbaumer, A., Reimer, E., Stern, R., Van Der Swaluw, E., Builtjes, P., 2012. Implementation and evaluation of pH-dependent cloud chemistry and wetdeposition in the chemical transport model REM-Calgrid. Atmos. Environ. 49 https://doi.org/10.1016/j.atmosenv.2011.10.069.

Banzhaf, S., Schaap, M., Kranenburg, R., Manders, A.M.M., Segers, A.J., Visschedijk, A.J. H., Denier van der Gon, H.A.C., Kuenen, J.J.P., van Meijgaard, E., van Ulft, L.H., Cofala, J., Builtjes, P.J.H., 2015. Dynamic model evaluation for secondary inorganic aerosol and its precursors over Europe between 1990 and 2009. Geosci. Model Dev. 8, 1047–1070. https://doi.org/10.5194/gmd-8-1047-2015.

Belis, C.A., Favez, O., Mircea, M., Diapouli, E., Manousakas, M.-I., Vratolis, S., Gilardoni, S., Paglione, M., Decesari, S., Mocnik, G., Mooibroek, D., Salvador, P., Takahama, S., Vecchi, R., Paatero, P., European Commission. Joint Research Centre., 2019. European Guide on Air Pollution Source Apportionment with Receptor Models : Revised Version 2019. Publ. Off. Eur. Union, Luxemb. https://doi.org/10.2760/439106. EUR 29816 EN.

Belis, C.A., Karagulian, F., Larsen, B.R., Hopke, P.K., 2013. Critical review and meta-analysis of ambient particulate matter source apportionment using receptor models in Europe. Atmos. Environ. https://doi.org/10.1016/j.atmosenv.2012.11.009.

Belis, C.A., Pernigotti, D., Pirovano, G., Favez, O., Jaffrezo, J.L., Kuenen, J., Denier van Der Gon, H., Reizer, M., Riffault, V., Alleman, L.Y., Almeida, M., Amato, F., Angyal, A., Argyropoulos, G., Bande, S., Beslic, I., Besombes, J.L., Bove, M.C., Brotto, P., Calori, G., Cesari, D., Colombi, C., Contini, D., De Gennaro, G., Di Gilio, A., Diapouli, E., El Haddad, I., Elbern, H., Eleftheriadis, K., Ferreira, J., Vivanco, M.G., Gilardoni, S., Golly, B., Hellebust, S., Hopke, P.K., Izadmanesh, Y., Jorquera, H., Krajsek, K., Kranenburg, R., Lazzeri, P., Lenartz, F., Lucarelli, F., Maciejewska, K., Manders, A., Manousakas, M., Masiol, M., Mircea, M., Mooibroek, D., Nava, S., Oliveira, D., Paglione, M., Pandolfi, M., Perrone, M., Petralia, E., Pietrodangelo, A., Pillon, S., Pokorna, P., Prati, P., Salameh, D., Samara, C., Samek, L., Saraga, D., Sauvage, S., Schaap, M., Scotto, F., Sega, K., Siour, G., Tauler, R., Valli, G., Vecchi, R., Venturini, E., Vestenius, M., Waked, A., Yubero, E., 2020. Evaluation of receptor and chemical transport models for PM10 source apportionment. Atmos. Environ. X 5, 100053. https://doi.org/10.1016/J.AEAOA.2019.100053.

Bessagnet, Bertrand, Menut, L., Curci, Gabriele, Hodzic, A., Guillaume, Bruno, Liousse, C., Moukhtar, Sophie, Pun, Betty, Seigneur, C., Schulz, Michael, Betty, ·, Schulz, Michaël, Bessagnet, B., Curci, G., Guillaume, B., Liousse, · C., Moukhtar, S., Pun, B., Seigneur, · C., Schulz, M., 2009. Regional modeling of carbonaceous aerosols over Europe—focus on secondary organic aerosols. J. Atmos. Chem. 61, 175–202. https://doi.org/10.1007/S10874-009-9129-2.

Borken-Kleefeld, J., Dallmann, T., Berlin, B., Brussels, |, San, Washington, F., 2018. White paper: remote sensing of motor vehicle exhaust emissions. accessible through. https://theicct.org/publication/remote-sensing-of-motor-vehicle-exhaust-emissions/.

Bove, M.C., Brotto, P., Cassola, F., Cuccia, E., Massabò, D., Mazzino, A., Piazzalunga, A., Prati, P., 2014. An integrated PM 2.5 source apportionment study: positive Matrix Factorisation vs. the chemical transport model CAMx. https://doi.org/10.1016/j.atmosenv.2014.05.039.

Bruns, E.A., El Haddad, I., Slowik, J.G., Kilic, D., Klein, F., Baltensperger, U., Prévôt, A.S. H., 2016. Identification of significant precursor gases of secondary organic aerosols from residential wood combustion. Sci. Rep. 61 (6), 1–9. https://doi.org/10.1038/srep27881, 2016.

Ciarelli, G., Aksoyoglu, S., Haddad, I. El, Bruns, E.A., Crippa, M., Poulain, L., Äijälä, M., Carbone, S., Freney, E., O'dowd, C., Baltensperger, U., Prévôt, A.S.H., 2017. Modelling winter organic aerosol at the European scale with CAMx: evaluation and source apportionment with a VBS parameterization based on novel wood burning smog chamber experiments. Atmos. Chem. Phys. 17, 7653–7669. https://doi.org/10.5194/acp-17-7653-2017.

Denier Van Der Gon, H.A.C., Bergström, R., Fountoukis, C., Johansson, C., Pandis, S.N., Simpson, D., Visschedijk, A.J.H., 2015. Particulate emissions from residential wood combustion in Europe - revised estimates and an evaluation. Atmos. Chem. Phys. https://doi.org/10.5194/acp-15-6503-2015.

ECMWF, 2021. IFS documentation CY47R3 - Part IV physical processes. ECMWF [WWW Document]. URL. https://www.ecmwf.int/en/elibrary/20198-ifs-documentation-cy47r3-part-iv-physical-processes, 3.21.22.

Fabbri, D., Torri, C., Simoneit, B.R.T., Marynowski, L., Rushdi, A.I., Fabiańska, M.J., 2009. Levoglucosan and other cellulose and lignin markers in emissions from burning of Miocene lignites. Atmos. Environ. 43, 2286–2295. https://doi.org/10.1016/j.atmosenv.2009.01.030.

Fagerli, H., Basart, S., CAMS 61 team, 2021. Evaluation of PM and its chemical components modelled by regional models in CAMS [WWW Document]. URL. https://atmosphere.copernicus.eu/sites/default/files/custom-uploads/CAMS-5thGA/day2/Fagerli H_Met Norway_Chemistry aerosol modelling.pdf, 12.17.21.

Fomba, K.W., van Pinxteren, D., Müller, K., Spindler, G., Herrmann, H., 2018. Assessment of trace metal levels in size-resolved particulate matter in the area of Leipzig. Atmos. Environ. 176, 60–70. https://doi.org/10.1016/J.ATMOSENV.2017.12.024.

Fountoukis, C., Nenes, A., 2007. ISORROPIAII: a computationally efficient thermodynamic equilibrium model for K+–Ca2+–Mg2+–NH4 +–Na+–SO42–NO3 –Cl–H2O aerosols. Atmos. Chem. Phys. 7, 4639–4659.

Harris, E., Sinha, B., van Pinxteren, D., Tilgner, A., Fomba, K.W., Schneider, J., Roth, A., Lee, T., Collett, J., Foley, S., Borrmann, S., ced role of transition metal ion catalysis during in-cloud oxidation of SO2. Science 340, 727–730. https://doi.org/10.1126/science.1230911.

He, H., Wang, Y., Ma, Q., Ma, J., Chu, B., Ji, D., Tang, G., Liu, C., Zhang, H., Hao, J., 2014. Mineral dust and NOx promote the conversion of SO2 to sulfate in heavy pollution days. Sci. Rep. 4, 4172. https://doi.org/10.1038/srep04172.

HEI, 2020. State of Global Air 2020. Special Report. Health Effects Institute, Boston, MA [WWW Document]. URL. https://www.stateofglobalair.org/sites/default/files/documents/2020-10/soga-2020-report.pdf.

Hendriks, C., Kranenburg, R., Kuenen, J., van Gijlswijk, R., Wichink Kruit, R., Segers, A., Denier van der Gon, H., Schaap, M., 2013. The origin of ambient particulate matter concentrations in the Netherlands. Atmos. Environ. 69, 289–303. https://doi.org/10.1016/j.atmosenv.2012.12.017.

Hopke, P.K., Cohen, D.D., 2011. Application of receptor modeling methods. Atmos. Pollut. Res. 2, 122–125. https://doi.org/10.5094/APR.2011.016.

Huang, Y., Deng, T., Li, Z., Wang, N., Yin, C., Wang, S., Fan, S., 2018. Numerical simulations for the sources apportionment and control strategies of PM2.5 over Pearl River Delta, China, part I: inventory and PM2.5 sources apportionment. Sci. Total Environ. 634, 1631–1644. https://doi.org/10.1016/J.SCITOTENV.2018.04.208.

Kolesar, K.R., Mattson, C.N., Peterson, P.K., May, N.W., Prendergast, R.K., Pratt, K.A., 2018. Increases in wintertime PM2.5 sodium and chloride linked to snowfall and road salt application. Atmos. Environ. 177, 195–202. https://doi.org/10.1016/J.ATMOSENV.2018.01.008.

Kranenburg, R., Segers, A.J.J., Hendriks, C., Schaap, M., 2013. Source apportionment using LOTOS-EUROS: module description and evaluation. Geosci. Model Dev. 6, 721–733. https://doi.org/10.5194/gmd-6-721-2013.

Kuenen, J., Dellaert, S., Visschedijk, A., Jalkanen, J.-P., Super, I., Denier van der Gon, H., 2021. CAMS-REG-v4: a state-of-the-art high-resolution European emission inventory for air quality modelling. Earth Syst. Sci. Data Discuss. 1–37. https://doi.org/10.5194/ESSD-2021-242.

Kuenen, J.J.P., Visschedijk, A.J.H., Jozwicka, M., Denier van der Gon, H.A.C., 2014. TNO-MACC_II emission inventory; a multi-year (2003–2009) consistent high-resolution European emission inventory for air quality modelling. Atmos. Chem. Phys. 14, 10963–10976. https://doi.org/10.5194/acp-14-10963-2014.

Manders, A., Visschedijk, A., Denier van der Gon, H., Kuenen, J., Timmermans, R., Schaap, M., Pfäfflin, F., Latt, C., Mahlau, A., Tautz, F., Wursthorn, H., Cuesta, A., Müller, T., van Pinxteren, D., Wiedensohler, A., 2021. Orientierende Erfassung von Black Carbon (BC) in Deutschland und Identifikation relevanter Quellen mit Chemie-Transport-Modellen. UBA report FKZ 3717 51 250 0, (in press).

Manders, A.M.M., Builtjes, P.J.H., Curier, L., Denier van der Gon, H.A.C., Hendriks, C., Jonkers, S., Kranenburg, R., Kuenen, J., Segers, A.J., Timmermans, R.M.A., Visschedijk, A., Wichink Kruit, R.J., Van Pul, W.A.J., Sauter, F.J., van der Swaluw, E., Swart, D.P.J., Douros, J., Eskes, H., van Meijgaard, E., van Ulft, B., van Velthoven, P., Banzhaf, S., Mues, A., Stern, R., Fu, G., Lu, S., Heemink, A., van Velzen, N., Schaap, M., 2017. Curriculum Vitae of the LOTOS-EUROS (v2.0) chemistry transport model. Geosci. Model Dev. 10, 4145–4173. https://doi.org/10.5194/gmd-10-4145-2017.

Marécal, V., Peuch, V.-H., Andersson, C., Andersson, S., Arteta, J., Beekmann, M., Benedictow, A., Bergström, R., Bessagnet, B., Cansado, A., Chéroux, F., Colette, A., Coman, A., Curier, R.L., Denier van der Gon, H.A.C., Drouin, A., Elbern, H., Emili, E., Engelen, R.J., Eskes, H.J., Foret, G., Friese, E., Gauss, M., Giannaros, C., Guth, J., Joly, M., Jaumouillé, E., Josse, B., Kadygrov, N., Kaiser, J.W., Krajsek, K., Kuenen, J., Kumar, U., Liora, N., Lopez, E., Malherbe, L., Martinez, I., Melas, D., Meleux, F., Menut, L., Moinat, P., Morales, T., Parmentier, J., Piacentini, A., Plu, M., Poupkou, A., Queguiner, S., Robertson, L., Rouïl, L., Schaap, M., Segers, A., Sofiev, M., Tarasson, L., Thomas, M., Timmermans, R., Valdebenito, Á., van Velthoven, P., van Versendaal, R., Vira, J., Ung, A., 2015. A regional air quality forecasting system over Europe: the MACC-II daily ensemble production. Geosci. Model Dev. 8, 2777–2813. https://doi.org/10.5194/gmd-8-2777-2015.

Mircea, M., Calori, G., Pirovano, G., Belis, C., 2020. European Guide on Air Pollution Source Apportionment for Particulate Matter with Source Oriented Models and Their Combined Use with Receptor Models. EUR 30082 EN, Publications Office of the EU, Luxembourg. https://doi.org/10.2760/470628, 2020, ISBN 978-92-76-10698-2, JRC119067.

Neusüß, C., Wex, H., Birmili, W., Wiedensohler, A., Koziar, C., Busch, B., Brüggemann, E., Gnauk, T., Ebert, M., Covert, D.S., 2002. Characterization and parameterization of atmospheric particle number-, mass-, and chemical-size distributions in central Europe during LACE 98 and MINT. J. Geophys. Res. Atmos. 107 https://doi.org/10.1029/2001JD000514. LAC 9-1.

Pinxteren, D. van, Fomba, K.W., Spindler, G., Müller, K., Poulain, L., Iinuma, Y., Löschau, G., Hausmann, A., Herrmann, H., 2016. Regional air quality in Leipzig, Germany: detailed source apportionment of size-resolved aerosol particles and comparison with the year 2000. Faraday Discuss 189, 291–315. https://doi.org/10.1039/C5FD00228A.

Pirovano, G., Colombi, C., Balzarini, A., Riva, G.M., Gianelle, V., Lonati, G., 2015. PM2.5 source apportionment in Lombardy (Italy): comparison of receptor and chemistry-transport modelling results. Atmos. Environ. C 56–70. https://doi.org/10.1016/J.ATMOSENV.2015.01.073.

Samaké, A., Jaffrezo, J.L., Favez, O., Weber, S., Jacob, V., Canete, T., Albinet, A., Charron, A., Riffault, V., Perdrix, E., Waked, A., Golly, B., Salameh, D., Chevrier, F., Miguel Oliveira, D., Besombes, J.L., Martins, J.M.F., Bonnaire, N., Conil, S., Guillaud, G., Mesbah, B., Rocq, B., Robic, P.Y., Hulin, A., Le Meur, S., Descheemaecker, M., Chretien, E., Marchand, N., Uzu, G., 2019. Arabitol, mannitol, and glucose as tracers of primary biogenic organic aerosol: the influence of environmental factors on ambient air concentrations and spatial distribution over France. Atmos. Chem. Phys. 19, 11013–11030. https://doi.org/10.5194/ACP-19-11013-2019.

Schaap, M., Kranenburg, R., Curier, L., Jozwicka, M., Dammers, E., Timmermans, R., 2013. Assessing the sensitivity of the OMI-NO2 product to emission changes across europe. Rem. Sens. 5, 4187–4208. https://doi.org/10.3390/rs5094187.

Schaap, M., van Loon, M., ten Brink, H.M., Dentener, F.J., Builtjes, P.J.H., 2004. Secondary inorganic aerosol simulations for Europe with special attention to nitrate. Atmos. Chem. Phys. 4, 857–874. https://doi.org/10.5194/acp-4-857-2004.

Seidel, D.J., Zhang, Y., Beljaars, A., Golaz, J.C., Jacobson, A.R., Medeiros, B., 2012. Climatology of the planetary boundary layer over the continental United States and Europe. J. Geophys. Res. Atmos. 117 https://doi.org/10.1029/2012JD018143.

Suarez-Bertoa, R., Astorga, C., 2018. Impact of cold temperature on Euro 6 passenger car emissions. Environ. Pollut. 234, 318–329. https://doi.org/10.1016/J.ENVPOL.2017.10.096.

Thunis, P., Degraeuwe, B., Pisoni, E., Trombetti, M., Peduzzi, E., Belis, C.A., Wilson, J., Clappier, A., Vignati, E., 2018. PM2.5 source allocation in European cities: a SHERPA modelling study. Atmos. Environ. 187, 93–106. https://doi.org/10.1016/J.ATMOSENV.2018.05.062.

Timmermans, R., Kranenburg, R., Manders, A., Hendriks, C., Segers, A., Dammers, E., Denier van der Gon, H., Schaap, M., Dammers, E., Zhang, Q., Wang, L., Liu, Z., 2017. Source apportionment of PM2.5 across China using LOTOS-EUROS. Atmos. Environ. 164 https://doi.org/10.1016/j.atmosenv.2017.06.003.

Tsyro, S.G., 2005. To what extent can aerosol water explain the discrepancy between model calculated and gravimetric PM10 and PM2.5? Atmos. Chem. Phys. 5, 515–532. https://doi.org/10.5194/ACP-5-515-2005.

Tuccella, P., Curci, G., Visconti, G., Bessagnet, B., Menut, L., Park, R.J., 2012. Modeling of gas and aerosol with WRF/Chem over Europe: evaluation and sensitivity study. J. Geophys. Res. Atmos. 117, 3303. https://doi.org/10.1029/2011JD016302.

US EPA, 2014. EPA Positive Matrix Factorization (PMF) 5.0 Fundamentals and User Guide [WWW Document]. URL. https://www.epa.gov/sites/default/files/2015-02/documents/pmf_5.0_user_guide.pdf, 10.28.21.

Uzan, L., Egert, S., Khain, P., Levi, Y., Vladislavsky, E., Alpert, P., 2020. Ceilometers as planetary boundary layer height detectors and a corrective tool for COSMO and IFS models. Atmos. Chem. Phys. 20, 12177–12192. https://doi.org/10.5194/ACP-20-12177-2020.

van Pinxteren, D., Mothes, F., Spindler, G., Fomba, K.W., Herrmann, H., 2019. Trans-boundary PM10: quantifying impact and sources during winter 2016/17 in eastern Germany. Atmos. Environ. 200, 119–130. https://doi.org/10.1016/j.atmosenv.2018.11.061.

Van Zanten, M.C., Sauter, F.J., Wichink Kruit, R.J., Van Jaarsveld, J.A., Van Pul, W.A.J., 2010. Description of the DEPAC module: dry deposition modelling with DEPAC GCN2010. RIVM Rep. 680180001/2010.

Viana, M., Kuhlbusch, T.A.J., Querol, X., Alastuey, A., Harrison, R.M., Hopke, P.K., Winiwarter, W., Vallius, M., Szidat, S., Prévôt, A.S.H., Hueglin, C., Bloemen, H., Wåhlin, P., Vecchi, R., Miranda, A.I., Kasper-Giebl, A., Maenhaut, W., Hitzenberger, R., 2008. Source apportionment of particulate matter in Europe: a review of methods and results. J. Aerosol Sci. 39, 827–849. https://doi.org/10.1016/j.jaerosci.2008.05.007.

Von Engeln, A., Teixeira, J., 2013. A planetary boundary layer height climatology derived from ECMWF reanalysis data. J. Clim. 26, 6575–6590. https://doi.org/10.1175/JCLI-D-12-00385.1.

Wagstrom, K.M., Pandis, S.N., Yarwood, G., Wilson, G.M., Morris, R.E., 2008. Development and application of a computationally efficient particulate matter apportionment algorithm in a three-dimensional chemical transport model. Atmos. Environ. 42, 5650–5659. https://doi.org/10.1016/j.atmosenv.2008.03.012.

Waked, A., Favez, O., Alleman, L.Y., Piot, C., Petit, J.-E., Delaunay, T., Verlinden, E., Golly, B., Besombes, J.-L., Jaffrezo, J.-L., Leoz-Garziandia, E., 2014. Source apportionment of PM10 in a north-western Europe regional urban background site (Lens, France) using positive matrix factorization and including primary biogenic emissions. Atmos. Chem. Phys. 14, 3325–3346. https://doi.org/10.5194/acp-14-3325-2014.

Walcek, C.J., 2000. Minor flux adjustment near mixing ratio extremes for simplified yet highly accurate monotonic calculation of tracer advection. J. Geophys. Res. Atmos. 105, 9335–9348.

Wang, J., Li, J., Ye, J., Zhao, J., Wu, Y., Hu, J., Liu, D., Nie, D., Shen, F., Huang, X., Huang, D.D., Ji, D., Sun, X., Xu, W., Guo, J., Song, S., Qin, Y., Liu, P., Turner, J.R., Lee, H.C., Hwang, S., Liao, H., Martin, S.T., Zhang, Q., Chen, M., Sun, Y., Ge, X., Jacob, D.J., 2020. Fast sulfate formation from oxidation of SO2 by NO2 and HONO observed in Beijing haze, 2020 Nat. Commun. 111 (11), 1–7. https://doi.org/10.1038/s41467-020-16683-x.

Wang, W., Liu, M., Wang, T., Song, Y., Zhou, L., Cao, J., Hu, J., Tang, G., Chen, Z., Li, Z., Xu, Z., Peng, C., Lian, C., Chen, Y., Pan, Y., Zhang, Y., Sun, Y., Li, W., Zhu, T., Tian, H., Ge, M., 2021. Sulfate formation is dominated by manganese-catalyzed oxidation of SO2 on aerosol surfaces during haze events. Nat. Commun. 121 12, 1–10. https://doi.org/10.1038/s41467-021-22091-6, 2021.

Wang, Y., Zhang, Qianqian, Jiang, J., Zhou, W., Wang, B., He, K., Duan, F., Zhang, Qian, Philip, S., Xie, Y., 2014. Enhanced sulfate formation during China's severe winter haze episode in January 2013 missing from current models. J. Geophys. Res. Atmos. 119 https://doi.org/10.1002/2013JD021426, 10,425-10,440.

Wang, Z.S., Chien, C.J., Tonnesen, G.S., 2009. Development of a tagged species source apportionment algorithm to characterize three-dimensional transport and transformation of precursors and secondary pollutants. J. Geophys. Res. Atmos. 114 https://doi.org/10.1029/2008JDO10846.

Weilenmann, M., Favez, J.Y., Alvarez, R., 2009. Cold-start emissions of modern passenger cars at different low ambient temperatures and their evolution over vehicle legislation categories. Atmos. Environ. 43, 2419–2429. https://doi.org/10.1016/J.ATMOSENV.2009.02.005.

Whitten, G., Hogo, H., Killus, J., 1980. The carbon bond mechanism for photochemical smog. Environ. Sci. Technol. 14, 14690–14700.

WHO, 2021. WHO global air quality guidelines [WWW Document]. URL. https://www.who.int/news-room/q-a-detail/who-global-air-quality-guidelines, 10.28.21.

Wichink Kruit, R.J., Schaap, M., Sauter, F.J., van Zanten, M.C., van Pul, W.A.J., 2012. Modeling the distribution of ammonia across Europe including bi-directional surface–atmosphere exchange. Biogeosciences 9, 5261–5277. https://doi.org/10.5194/bg-9-5261-2012.

Yan, C., Zheng, M., Sullivan, A.P., Shen, G., Chen, Y., Wang, S., Zhao, B., Cai, S., Desyaterik, Y., Li, X., Zhou, T., Gustafsson, Ö., Collett, J.L., 2018. Residential coal combustion as a source of Levoglucosan in China. Environ. Sci. Technol. 52, 1665–1674. https://doi.org/10.1021/acs.est.7b05858.

Zhang, L., 2001. A size-segregated particle dry deposition scheme for an atmospheric aerosol module. Atmos. Environ. 35, 549–560. https://doi.org/10.1016/S1352-2310(00)00326-5.